Global Riemann Solver and Front Tracking Approximation of Three-Component Gas Floods

Saeid Khorsandi[1], Wen Shen[2] and Russell T. Johns[3]

[1] Department of Energy and Mineral Engineering, Penn State University.
Email: sxk482@psu.edu.

[2] Mathematics Department, Penn State University. Email: wxs27@psu.edu.

[3] Department of Energy and Mineral Engineering, Penn State University.
Email: rjohns@psu.edu.

June 18, 2015

Abstract

We study a 2×2 system of non-strictly hyperbolic conservation laws arising in three–component gas flooding for enhanced oil recovery. The system is not strictly hyperbolic. In fact, along a curve in the domain one family is linearly degenerate, and along two other curves the system is parabolic degenerate. We construct global solutions for the Riemann problem, utilizing the splitting property of thermo-dynamics from the hydro-dynamics. Front tracking simulations are presented, using the global Riemann Solver.

1   The Three-Component Gas Flooding Model

We consider a simplified compositional displacement model for a three-component system at constant temperature and pressure [11],

(1.1) $\qquad (C_1)_t + (F_1(C_1, C_2))_x = 0\,, \qquad (C_2)_t + (F_2(C_1, C_2))_x = 0\,,$

associated with initial data

(1.2) $\qquad C_1(0, x) = \bar{C}_1(x)\,, \qquad C_2(0, x) = \bar{C}_2(x)\,.$

The independent variables (t, x) are normalized such that the overall velocity is 1. Here C_i is the overall i^{th} component volume fraction, and F_i is the overall i^{th} component flux. For the third component, we trivially have

$$C_3 = 1 - C_1 - C_2\,, \qquad F_3 = 1 - F_1 - F_2\,.$$

The couplet (C_1, C_2) takes values in a triangular domain

$$D = \{(C_1, C_2) \mid C_1 \geq 0, C_2 \geq 0, 1 - C_1 - C_2 > 0\}\,.$$

For the phase behaviors that are considered in this paper, there exists a subset $D_2 \subset D$, referred to as the two-phase region, where the fluid splits into two phases, the liquid and the gaseous phases. In the single phase region $D_1 = D \setminus D_2$, we trivially have

$$F_1(C_1, C_2) = C_1\,, \qquad F_2(C_1, C_2) = C_2\,.$$

1

We briefly derive the equations in the two-phase region. We denote by c_{il} and c_{ig} the composition of component i in the liquid and gaseous phases, respectively. For $(C_1, C_2) \in D_2$ the compositions c_{il} and c_{ig}, together with the liquid phase saturation S, satisfy the following equations,

$$(1.3) \quad C_i = c_{il}S + c_{ig}(1-S), \quad F_i = c_{il}f + c_{ig}(1-f), \quad i = 1, 2, \quad \sum_{i=1}^{3} c_{il} = \sum_{i=1}^{3} c_{ig} = 1.$$

Here $f = f(S, C_1, C_2)$ is the fractional flow of liquid, and S takes values between 0 and 1 in the two-phase region. Typically, for given (C_1, C_2), the mapping $S \mapsto f$ is S-shaped with an inflection point. The K-values, defined as

$$(1.4) \qquad\qquad\qquad K_i \doteq \frac{c_{ig}}{c_{il}}, \qquad i = 1, 2, 3,$$

are determined by a phase behavior model and can either be taken as constant or a function of (C_1, C_2) (e.g. [31]). For given (C_1, C_2) and K_i, one can calculate c_{il}, c_{ig} and S by simultaneous solution of (1.3), and (1.4). This simultaneous solution of equations is called a flash calculation in the engineering literature and can be complicated for the systems with more than three components [19]. In case of composition dependent K-values, the equilibrium compositions are determined by an iterative procedure [29]. Next, the results of flash calculations are used to calculate f and F_i.

For fixed (c_{il}, c_{ig}) for $i = 1, 2$, the values (C_1, C_2) are linear functions of S. In the phase coordinate (C_1, C_2), as S varies from 0 to 1, the trajectory of the couplet (C_1, C_2) is the straight line connecting the equilibrium points (c_{1g}, c_{2g}) and (c_{1l}, c_{2l}). When $S = 0$, we have $(C_1, C_2) = (c_{1l}, c_{2l})$, and when $S = 1$, we have $(C_1, C_2) = (c_{1g}, c_{2g})$. These lines are called *tie-lines*. The curves of the end-points of these tie-lines, namely the points (c_{1g}, c_{2g}) and (c_{1l}, c_{2l}), form the boundaries of the two-phase region. One may artificially extend the tie-lines into single-phase region. We assume that the tie-lines do not intersect in the domain D, such that any point $(C_1, C_2) \in D$ lies on one unique tie-line. See Figure 1 (left) for a plot of the two-phase region and the tie-lines.

It is well-known that the system of conservation laws (1.1) is not hyperbolic. There exist two curves in D_2 where the two eigenvalues as well as the two eigenvectors of the Jacobian matrix of the flux function coincide, and the system is singular. On the other hand, the system (1.1) has many interesting properties. Indeed, one family of integral curves of the Jacobian matrix are straight lines, which coincide exactly with the tie-lines. This motivates a parametrization of the tie-lines and a variable change of the unknowns. Without loss of generality, we retain the equation for C_1 in (1.1) and write

$$(1.5) \qquad\qquad C = C_1, \qquad F = F_1, \qquad C_2 = \alpha C + \beta, \qquad F_2 = \alpha F + \beta,$$

where α and β are defined as

$$(1.6) \qquad\qquad\qquad \alpha = \frac{c_{2l} - c_{2g}}{c_{1l} - c_{1g}}, \qquad \beta = c_{2g} - \alpha c_{1g}.$$

Here α indicates the slope of a tie line, and β its interception point with the line $C_1 = 0$. Under the assumption that the tie lines do not intersect with each other in the domain D, one may parametrize the tie lines with β [16, 18], and consider $\alpha = \alpha(\beta)$. Treating (C, β) as the unknowns, the system (1.1) becomes

$$(1.7) \qquad C_t + F(C, \beta)_x = 0, \qquad C(\alpha(\beta))_t + \beta_t + F(C, \beta)(\alpha(\beta))_x + \beta_x = 0.$$
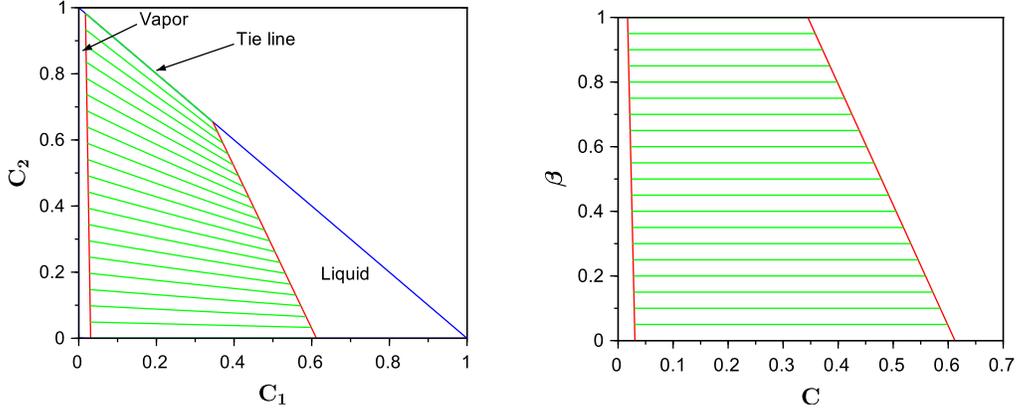
Figure 1: Illustration of three-component phase diagram with constant K-values $(K_1, K_2, K_3) = (0.05, 1.5, 2.5)$. Left plot uses the (C_1, C_2) coordinate, which the right plot uses the (C, β) coordinate. The two red curves are the boundary of the two-phase region, and green lines are tie lines.

associated with the initial data

$$(1.8) \qquad C(0, x) = \bar{C}(x), \qquad \beta(0, x) = \bar{\beta}(x).$$

The tie lines are now horizontal lines in the (C, β)-phase plane, illustrated in Figure 1 (right).

Construction of solutions of the Riemann problems can be challenging for three-component systems [23]. In [32], the following Lagrangian coordinates (φ, ψ) was introduced,

$$(1.9) \qquad \varphi_x = -C, \quad \varphi_t = F, \qquad \text{and} \quad \psi = x - t.$$

Straight computation leads to the following system

$$(1.10) \qquad \left(\frac{C}{F - C} \right)_\varphi - \left(\frac{1}{F - C} \right)_\psi = 0,$$

$$(1.11) \qquad \beta_\varphi + \alpha(\beta)_\psi = 0.$$

The thermodynamics process described in (1.11) is decoupled from the fractional flow in (1.10) (also known as the hydro-dynamics). Solutions of Riemann problems could be rather simply constructed if this coordinate change were well-defined in the whole domain D. In fact, given left and right states (C^L, β^L) and (C^R, β^R), one could first solve (1.11) for β, then substitute the solution into (1.10), and solve a scalar conservation law with possibly discontinuous coefficients.

Unfortunately, (1.10)-(1.11) does not offer this possibility, since the quantities $\frac{C}{F-C}$ and $\frac{1}{F-C}$ do not allow a single-valued function between them. Furthermore, the coordinate change is only valid in the set when $F > C$. Indeed, let J be the Jacobian matrix for this coordinate change,

$$J \doteq \frac{\partial(\varphi, \psi)}{\partial(t, x)} = \begin{pmatrix} F & -C \\ -1 & 1 \end{pmatrix}, \qquad \text{so} \quad \det(J) = F - C.$$

Thus $\det(J) = 0$ when $F = C$, and the coordinate change is not valid there. Furthermore, $\det(J) < 0$ when $F < C$, so the resulting conservation laws are not equivalent to the original

3

ones. See Wagner [38] for a discussion on the equivalence between the Eulerian and Lagrangian coordinates for the Euler's equations of gas dynamics.

If $F < C$, we define different Lagrangian coordinates,

$$(1.12) \qquad \tilde{\varphi}_x = C, \quad \tilde{\varphi}_t = -F, \qquad \text{and} \quad \tilde{\psi} = x - t.$$

The Jacobian matrix $\tilde{J}$ for this coordinate change is

$$\tilde{J} \doteq \frac{\partial(\tilde{\varphi}, \tilde{\psi})}{\partial(t, x)} = \begin{pmatrix} -F & C \\ -1 & 1 \end{pmatrix}, \qquad \text{so} \quad \det(\tilde{J}) = C - F > 0.$$

Formal computation leads to the following system:

$$(1.13) \qquad \left(\frac{C}{C-F}\right)_{\tilde{\varphi}} + \left(\frac{1}{C-F}\right)_{\tilde{\psi}} = 0,$$

$$(1.14) \qquad \beta_{\tilde{\varphi}} - \alpha(\beta)_{\tilde{\psi}} = 0.$$

Nevertheless, the splitting nature can still be utilized in both numerical computation and theoretical analysis. In this paper we construct solutions for global Riemann problems, taking advantage of the splitting property. Given left and right states (C^L, β^L) and (C^R, β^R), we would first solve for β, using either (1.11) if $F > C$, and (1.14) if $F < C$. This gives us a-priori information on waves connecting different tie-lines. The global Riemann solver for (1.7) can be constructed based on this information. The Riemann solver is then used to generate piecewise constant front tracking approximate solutions.

The construction of the Riemann solver is closely related to that of a scalar conservation law with discontinuous coefficients. Additional difficulties arise from the lack of strict hyperbolicity. It is well-known that for hyperbolic conservation laws some additional constraint is needed on discontinuities in the weak solution to ensure uniqueness. These constraints are referred to as entropy (or admissible) conditions, and the corresponding shocks as "admissible shocks". Well-known conditions include the Kruzhkov condition [24] for scalar conservation laws, Lax condition [27] for genuinely nonlinear systems, Liu condition [28] which also allows certain local linear degeneracies, and the vanishing viscosity approach by Bianchini & Bressan [2, 3] for scalar equations and for strictly hyperbolic systems. These conditions are equivalent for the same system where ever the conditions are applicable.

For non-hyperbolic systems, there has not been a unified entropy condition. A generalized Lax entropy condition was proposed by Keyfitz & Kranzer [22] for a model of elasticity. In connection with scalar conservation laws with discontinuous flux function, Gimse & Risebro [9, 10] introduced the shortest-path criterion, and proved its equivalence to the vanishing viscosity limit. We remark that these two entropy conditions are different for certain cases of Riemann problems, and would give very different entropy weak solutions. In this paper, we adopt the Gimse & Risebro admissible condition.

Riemann problems for this type of non-strictly hyperbolic systems arising in simulation of multiphase flow in porous media have been studied by many authors. Buckley and Leveret [4] first developed the scalar conservation law for the water flooding which is a two phase flow without mass transfer between phases. Later, Helfferich, Hirasaki and Pope extended the models to the more complicated processes such as polymer flooding and gas flooding [11, 12, 33]. For the polymer flooding models, Johansen, Tveito and Winther [14, 15, 17] constructed global Riemann solvers for an adsorptive model under various assumptions, and conducted

4

numerical simulations with front tracking. Isaacson and Temple [13] studied the Riemann problem of a non-adsorptive polymer flooding model, and constructed approximation solutions using Glimm's Randon Choice. Using the generalized Langmuir isotherm for the adsorption functions in multi-component chromatography, Riemann solutions were constructed by Rhee, Aris & Amundson in a celebrated paper [34], taking advantage of the fact that the system is Temple class [37]. Dahl, Johansen, Tveito & Winther [5] constructed Riemann solutions for a model of multi-component displacement in two-phase flow without mass transfer between phases. Juanes and Lie [21, 26] applied the Riemann solver of Isaacson and Temple to three component water alternating gas flooding model yet without mass transfer between phases.

The mass transfer between phases makes the partially miscible gas flooding Riemann problem complex and the complexity increases as the number of components and phases increase. Helfferich [11] identified paths for connecting waves of different families for such complex systems, allowing an elegant but heuristic construction for solutions of Riemann problem. However, an exact global Riemann solver is unfortunately more complicated than what Helfferich [11] predicted. The two-component displacements can be modeled with scalar conservation laws and Johns developed a front tracking algorithm for such systems [18]. The global Riemann solver for three component systems is complicated. Instead of developing a general Riemann solver, many authors have solved the Riemann problems for specific boundary conditions [18, 23, 25, 35]. The structure of solution is very different for different boundary condition and fluid phase behavior.

Gas flooding displacements are usually modeled with more than three components [7] and the solutions of Riemann problems of such systems are very complicated [20, 30]. The solution can be constructed as several consecutive three component systems [20], however the solution is still complex. The other approach to simplify the solutions is to use the decoupled nature of thermodynamics in the gas flooding problem such that the solution can be constructed by calculating intersecting tie lines [20, 39]. However, the assumptions of such solutions are invalid for some fluids [1] and solutions of intersecting tie lines can be non-unique [40]. The current work presents a global Riemann solver for three-component systems by extending the splitting approach developed in [8, 32]. The splitting of hydrodynamics from tie lines greatly simplifies the solution to gas flood problems.

The rest of the paper is organized as follows. In Section 2 we give some basic analysis, the precise assumptions on the model, along with the main results. Wave behaviors of both families are analyzed in detail in Section 3. In Section 4 we connect various waves and construct global existence of solutions for Riemann Problems. Some numerical simulation using wave front tracking algorithm is performed and the results presented Section 5, to solve the three-component slug injection problem with mass transfer between phases. Finally, some concluding remarks are provided at the end of the paper.

2   Basic analysis, precise assumptions, and the main results

We assume that in the phase plan (C_1, C_2), no two tie-lines intersect in the domain D. Using (1.6) and (1.3), we have

$$(2.1) \qquad \alpha(\beta) = \frac{\beta(1 - K_2)(K_1 - K_3)}{\beta(K_1 - 1)(K_2 - K_3) + (K_2 - K_1)(1 - K_3)}.$$

Computation shows that the intersection point of any two tie-lines is outside the domain D if the K-values satisfy one of the following conditions

(2.2) $$K_3 < K_2 < 1 < K_1, \qquad \text{or} \qquad K_1 < 1 < K_2 < K_3.$$

Such conditions are called strictly ordered K-values in the petroleum engineering literature [30]. This labeling of components can be different from the conventional ordering of components based on molecular weight. Under the assumption (2.2), every couplet $(C_1, C_2) \in D$ corresponds to a unique couplet (C, β).

Defining the unknown vector

(2.3) $$u \doteq (C, \beta)^t,$$

the system (1.7) can be written into the quasi-linear form

(2.4) $$u_t + A(u)u_x = 0, \qquad \text{where} \quad A(u) = \begin{bmatrix} F_C & F_\beta \\ 0 & \frac{F\alpha'(\beta)+1}{C\alpha'(\beta)+1} \end{bmatrix}.$$

The matrix $A(u)$ has the following eigenvalues and right-eigenvectors

(2.5) $$\lambda^C = F_C, \qquad r^C = \begin{bmatrix} 1 \\ 0 \end{bmatrix}, \qquad \lambda^\beta = \frac{F + [\alpha'(\beta)]^{-1}}{C + [\alpha'(\beta)]^{-1}}, \qquad r^\beta = \begin{bmatrix} -F_\beta \\ F_C - \lambda^\beta \end{bmatrix}.$$

Here the labeling of the two families are not with respect to wave speed. We referred to λ^C and λ^β as the eigenvalues for the tie-line and non tie-line families, respectively. Sample integral curves for the β-eigenvectors (nontie-line paths) are plotted in Fig. 2. The values $(C = -[\alpha'(\beta)]^{-1}, \beta)$ gives the envelope curve of the tie lines.

A computation on the directional derivative of λ^β in the direction r^β gives

(2.6) $$\nabla \lambda^\beta \cdot r^\beta = \frac{1}{(C\alpha'(\beta)+1)^2} \alpha''(\beta)(F_C - \lambda^\beta)(F - C).$$

This indicates that along the curve $F = C$, the eigenvalue λ^β remains constant. This curve lies between the two groups of integral curves (see the green curve in Fig. 2), and is a β-integral curve (see the proof of Lemma 3.2), along which the β-family is linearly degenerate. This curve is referred to as the equi-velocity curve, and we will use the abbreviation EVC throughout this paper.

Furthermore, (2.6) also indicates that along a β-integral curve, the derivative of λ^β changes sign at the point where $F_C - \lambda^\beta = 0$. The S-shape of the map $C \mapsto F(C, \beta)$ for any fixed β gives rise to exactly two such points in the two-phase region. At these points we also have

$$\lambda^C = \frac{\partial F}{\partial C} = \frac{F + [\alpha'(\beta)]^{-1}}{C + [\alpha'(\beta)]^{-1}} = \lambda^\beta, \qquad r^C = r^\beta = (1, 0)^t,$$

i.e., the two eigenvalues as well as the two eigenvectors coincide, so the system is parabolic degenerate. These points are referred to as the *umbilical points*. As β varies, we have two curves in the two-phase region, one on each side of the EVC, where the system is degenerate.

For the convenience of our analysis, we introduce a new functional. For fixed β and parameter a, we define a function $\mathcal{F}(C; \beta, a)$ as

(2.7) $$\mathcal{F}(C; \beta, a) \doteq \frac{F(C, \beta) + a}{C + a}.$$

6
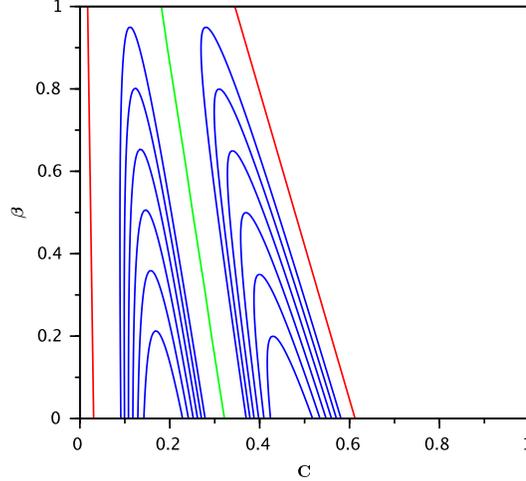
Figure 2: Integral curves for the β-family in the phase plane (C, β), corresponding to the case in Fig. 1. Here, the red curves are the boundary of the two-phase region and are called binodal curves.

This function takes the value of the slope between the point $(-a, -a)$ and (C, F), see Figure 3 plots (a) and (b) for an illustration. For $a = [\alpha'(\beta)]^{-1}$ the function takes the values of λ^β. Note that for fixed β and a, the function $C \mapsto \mathcal{F}$ reaches its minimum and maximum values at $C_{\min}$ and $C_{\max}$ respectively, where the lines $(-a, -a)$–$(C_{\min}, F(C_{\min}))$ and $(-a, -a)$–$(C_{\max}, F(C_{\max}))$ are tangent to the graph of $F(C, \beta)$ in plot (a).

We now state the precise assumptions on the functions $F(C, \beta)$ and $\alpha(\beta)$ as follows.

A1. The map $\beta \mapsto \alpha$ is $\mathbb{C}^2$ either strictly concave $\alpha'' < 0$ or strictly convex $\alpha'' > 0$.

A2. The function $F(C, \beta)$ is $\mathbb{C}^2$. For any fixed β, the map $C \mapsto F$ is an S-shaped function with a unique inflection point. In the two-pause region, the map $C \mapsto F$ is strictly convex $F_{CC} > 0$ on the left of the inflection point, and strictly concave $F_{CC} < 0$ on the right of the inflection point.

A3. The length of tie-lines in the two-phase region is a monotone function in β, such that the followings hold. Between any two tie-lines, say with β^1 and β^2, either everything point on the line $\beta = \beta^1$ can be connected to some point on the line $\beta = \beta^2$ by at least one β-integral curve, or every point on the line $\beta = \beta^2$ can be connected to some point on the line $\beta = \beta^1$ by at least one β-integral curve.

We remark that, the explicit expression for integral curves of the systems with constant K-values shows the same behavior as (A3) [6]. However, for phase behavior with composition dependent K-values, if the order of K-values changes, (A3) may not hold [23].

Below is the main result of the paper.

Theorem 2.1. *The Riemann problem for (1.7) has a unique global solution for any Riemann data u^L and u^R. Furthermore, in the phase plane (C, β), the path of the β-wave lies on the same side of the EVC as the left state u^L.*
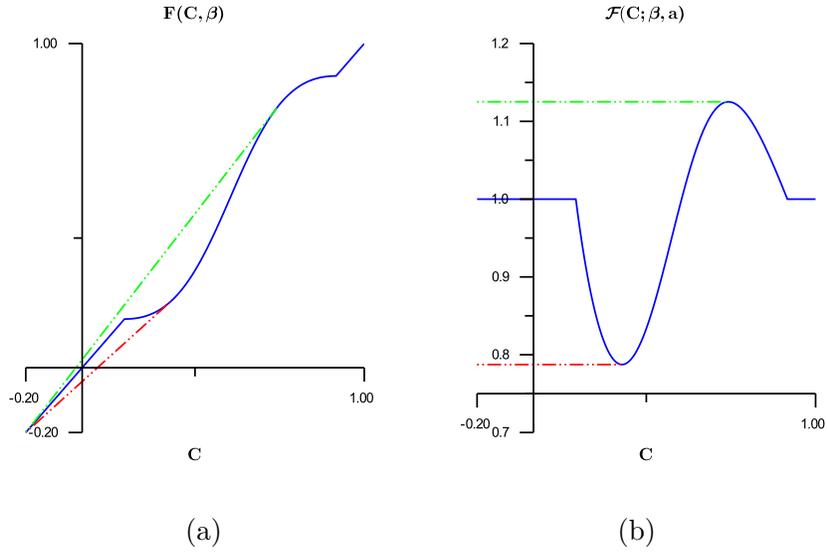
Figure 3: Functions $F(C, \beta)$ and $\mathcal{F}(C; \beta, a)$. $a = 0.2$ on the left plot.

3 Basic Wave Behavior

3.1 The C-waves

We first recall the Liu admissibility condition [28] for shocks. Let $u^+ = S_\beta(\sigma)(u^L)$ for some $\sigma \in \mathbb{R}$ be a point on the β-shock curve through the left state u^L. We say that the shock with left and right state (u^L, u^+) *satisfies the Liu admissibility condition* provided that its speed is less or equal to the speed of every smaller shock, joining u^L with an intermediate state $u^* = S_\beta(s)(u^L)$, $s \in [0, \sigma]$.

When β is a constant, then two equations in (1.7) are the same. This scalar conservation law, where C is the unknown, has a Buckley-Leverett type flux function [4]. Solutions of Riemann problems are well-understood, see for example [36]. We referred the waves there as C-waves. Let (C^L, β) and (C^R, β) be the left and right states, the solution of the Riemann problem is constructed such that all shocks satisfy the Liu admissibility condition, and it could consist of composite waves. To construct these wave, if $C^L > C^R$, we make the concave upper envelope of the flux function, while if $C^L < C^R$, we make the lower convex envelope, and the C-waves are constructed accordingly. See Figure 4 for an illustration. All C-shocks satisfy the Liu admissible condition.

3.2 The β-waves

The waves that connect two different tie lines, i.e., two different β values, are referred as β-waves.

8
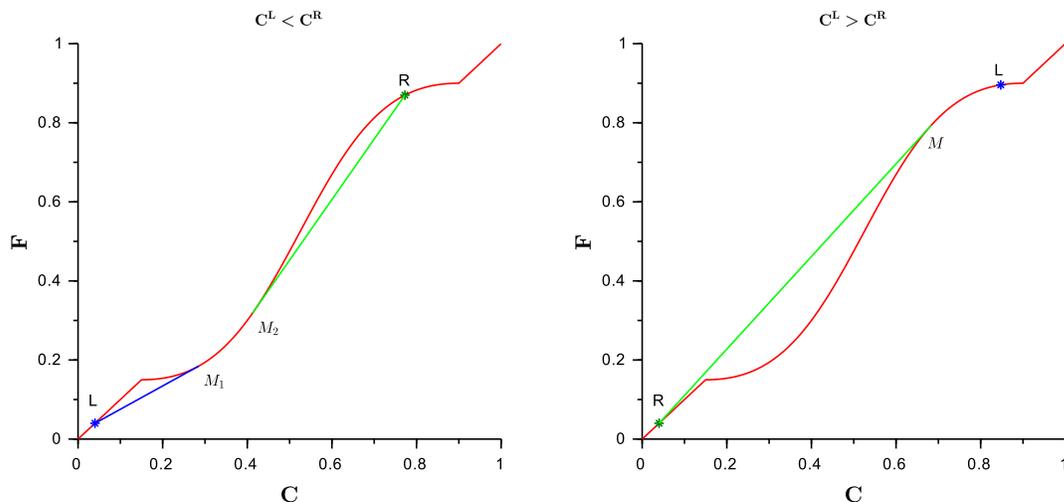
Figure 4: Solutions to Riemann problems for C-waves. Left: If $C^L < C^R$, the lower convex envelope L-M_1-M_2-R gives a shock L-M_1, a rarefaction fan M_1-M_2 and a shock M_2-R. Right: If $C^L > C^R$, the upper concave envelope L-M-R gives a rarefaction fan L-M and then a shock M-R.

3.2.1 The β-shocks

We recall the Lax admissible condition for shocks. Along a shock curve of the ith family in the (x,t) plan, the nearby characteristics of the same family must merge into the shock. For scalar conservation law with general flux function, Lax condition is necessary but not sufficient. However, if the flux is strictly convex or concave, these two conditions are equivalent.

In our model, the system is degenerate along two curves, therefore it is difficult to define admissible shock loci across these degenerate curves. Indeed, shock locus might be discontinuous, thus it is unclear how to apply the Liu condition. Since the β-family is strictly convex or concave, we apply instead the Lax admissible condition. We remark that the Lax condition, combined with the minimum jump condition [9] will eventually yield the unique solution for Riemann problems, proved in Section 4.

For a β-shock, the C value is not constant across the shock. We first show that the Lax admissibility condition for β-shocks for the system (1.7) is equivalent to the same condition for the scalar equation (1.11) or (1.14), for $F > C$ or $F < C$ respectively.

Lemma 3.1. *Let (C, β) be piecewise continuous solution of (1.7), and let (C^L, β^L) and (C^R, β^R) be the left and right state of the a β-shock that satisfies the Rankine-hugoniot condition. Then, we have*

$$(3.1) \qquad \text{sign}\left(F(C^L, \beta^L) - C^L\right) = \text{sign}\left(F(C^R, \beta^R) - C^R\right).$$

Furthermore, the followings hold.

- *If $F(C^L, \beta^L) = C^L$, then $F(C^R, \beta^R) = C^R$, and this shock is a contact discontinuity.*

- *If $F(C^L, \beta^L) > C^L$ and $F(C^R, \beta^R) > C^R$, then the shock (C^L, β^L)-(C^R, β^R) satisfies the Lax condition if and only if (β^L, β^R) is a shock for (1.11) that satisfies the Lax condition.*

9

- If $F(C^L, \beta^L) < C^L$ and $F(C^R, \beta^R) < C^R$, then the shock (C^L, β^L)-(C^R, β^R) satisfies the Lax condition if and only if (β^L, β^R) is a shock for (1.14) that satisfies the Lax condition.

Proof. Let (C^L, β^L) and (C^R, β^R) be the left and right state of a β-shock, respectively, and let σ_β be the shock speed. The Rankine-Hugoniot condition requires

$$(3.2) \qquad \sigma_\beta(C^L - C^R) \;=\; F^L - F^R,$$

$$(3.3) \qquad \sigma_\beta(\alpha^L C^L + \beta^L - \alpha^R C^R - \beta^R) \;=\; \alpha^L F^L + \beta^L - \alpha^R F^R - \beta^R.$$

Here we used the short hands

$$F^L = F(C^L, \beta^L), \quad F^R = F(C^R, \beta^R), \qquad \alpha^L = \alpha(\beta^L), \quad \alpha^R = \alpha(\beta^R).$$

We can eliminate C^R or C^L by multiplying (3.2) with suitable factor and subtract the remaining equation from (3.3). Simple calculation gives

$$(3.4) \qquad \sigma_\beta = \frac{F^L + \tilde\sigma_\beta^{-1}}{C^L + \tilde\sigma_\beta^{-1}} = \frac{F^R + \tilde\sigma_\beta^{-1}}{C^R + \tilde\sigma_\beta^{-1}}, \qquad \text{where} \qquad \tilde\sigma_\beta = \frac{\alpha^L - \alpha^R}{\beta^L - \beta^R}.$$

Note that $\tilde\sigma_\beta$ is the Rankine-Hugoniot speed for (1.11) in the Lagrangian coordinate.

In the phase plane (C_1, C_2), the two tie-lines associated with β^L and β^R intersect at the point where $C_1 = -\tilde\sigma_\beta^{-1}$. Under our assumption, this point lies outside the domain D, either to the left or to the right of D. Assuming it is on the left such that $-\tilde\sigma_\beta^{-1} < 0$, we illustrate the geometric meaning of (3.4), in Figure 5 for an illustration. This clearly implies (3.1). The case where the intersection point is on the right of D is completely similar.
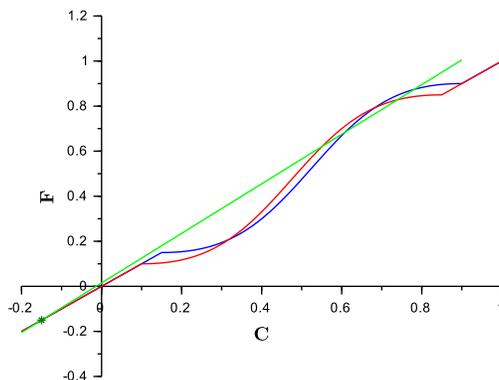
Figure 5: Illustration for β shock. Here the red and blue curves are graphs for F^L and F^R, and $*$ is the point $(-\tilde\sigma_\beta^{-1}, -\tilde\sigma_\beta^{-1})$. The green line has slope σ_β. Then, the C^L, C^R must be selected from the corresponding graphs of F^L and F^R that intersect with the green line.

For the rest of the proof we only consider the case $-\tilde\sigma_\beta^{-1} < 0$. If $F^L = C^L$, i.e., the left state is on the EVC, then by (3.4) we have $\sigma_\beta = 1$, and we must have $F^R = C^R$ for every state (C^R, β^R) that could be connected to (C^L, β^L) with a β-shock. Thus the right state must also lie on the EVC. Along such a shock curve, the second eigenvalue $\lambda_\beta \equiv 1$, and the β-family is linearly degenerate. This discontinuity is actually a contact discontinuity, proved later in Lemma 3.2.

Otherwise if $F^L > C^L$, by (3.4) we have $\sigma_\beta > 1$, and therefore $F^R > C^R$. In order to show the equivalence of the two Lax conditions, i.e.,

$$\alpha'(\beta^L) > \tilde{\sigma}_\beta > \alpha'(\beta^R) \qquad \Longleftrightarrow \qquad \lambda^\beta(C^L, \beta^L) > \sigma_\beta > \lambda^\beta(C^R, \beta^R),$$

it suffices to show that the mapping

$$s \mapsto \frac{F + s^{-1}}{C + s^{-1}}$$

is strictly increasing for any fixed F and C with $F > C$. This fact can be easily verified.

The proof for the case $F^L < C^L$ is completely similar. The same results can be shown similarly for the case where the intersection point of the two tie-lines is on the right of D. $\qquad \square$

3.2.2 β-rarefactions.

A β-rarefaction wave will connect (C^L, β^L) to (C^R, β^R) along the integral curves of the β-field. Similar to Lemma 3.1, we have the following Lemma.

Lemma 3.2. *Consider piecewise continuous solutions of (1.7), and let (C^L, β^L) and (C^R, β^R) be the left and right states of a β-rarefaction wave in the two phase region. Then, we have*

(i) *If $F(C^L, \beta^L) = C^L$, then $F(C^R, \beta^R) = C^R$, and this wave is a contact discontinuity.*

(ii) *If $F(C^L, \beta^L) > C^L$ then $F(C^R, \beta^R) > C^R$, and (β^L, β^R) is a rarefaction wave for (1.11).*

(iii) *If $F(C^L, \beta^L) < C^L$, then $F(C^R, \beta^R) < C^R$, and (β^L, β^R) is a rarefaction wave for (1.14).*

Proof. In the phase plane (C, β), the β-rarefaction curves are the integral curves of the second eigenvector of the Jacobian matrix of the flux function for (1.6), given in (2.5). Let $s \mapsto R(s)(C^L, \beta^L)$ denote a β-rarefaction curve initiated at (C^L, β^L) where s is the parametrization of the curve such that $R(0)(C^L, \beta^L) = (C^L, \beta^L)$. We first show that the EVC is an integral curve. It suffices to show that $(C_s, \beta_s)^t$ is parallel to the eigenvector r^β. Indeed, taking partial derivative in s of the equation $F(C, \beta) = C$, we get

$$F_C C_s + F_\beta \beta_s - C_s = 0, \qquad \text{i.e.,} \qquad \begin{pmatrix} C_s \\ \beta_s \end{pmatrix} \cdot \begin{pmatrix} F_C - 1 \\ F_\beta \end{pmatrix} = 0.$$

If $F = C$, we have $\lambda_\beta = 1$ and so $r^\beta = (-F_\beta, F_C - 1)^t$. Thus $(C_s, \beta_s)^t$ is parallel to r^β, as claimed. This proves (i). By the uniqueness of the integral curves, (ii) and (iii) follows, completing the proof. $\qquad \square$

4 Global solutions of Riemann problems

The solution of a Riemann problem is the key building block in a front tracking algorithm. In this section we construct solutions for Riemann problems with any Riemann data, taking advantage of the splitting property in the Lagrangian coordinates.

4.1 Connecting C-waves with β-shock

Connecting C-waves with a β-shock results in the Riemann problem for a scalar conservation law with discontinuous coefficient function. Let $u^L = (C^L, \beta^L)^t$ and $u^R = (C^R, \beta^R)^t$ be the left and right states of the Riemann data, and assume that β^L-β^R is connected by a single β-shock. We consider an implicit Riemann problem for a scalar conservation law with discontinuous flux function,

$$(4.5) \qquad C_t + \hat{F}(C, x)_x = 0, \qquad \hat{F}(C, x) = \begin{cases} F^L(C) = F(C, \beta^L), & x > \sigma_\beta t, \\ F^R(C) = F(C, \beta^R), & x < \sigma_\beta t, \end{cases}$$

with initial Riemann data

$$(4.6) \qquad C(0, x) = \begin{cases} C^L, & x > 0, \\ C^R, & x < 0. \end{cases}$$

Note that the wave speed σ_β is unknown, and it will be determined after the Riemann problem is solved. This feature makes the Riemann problem solver implicit.

In order to remove the implicit feature, we recall the definition of the function $\mathcal{F}(C; \beta, a)$ in (2.7). Given β^L and β^R, we define the $\mathcal{F}$ functions

$$(4.7) \qquad \mathcal{F}^L = \mathcal{F}(C; \beta^L, \tilde{\sigma}_\beta), \qquad \mathcal{F}^R = \mathcal{F}(C; \beta^R, \tilde{\sigma}_\beta), \quad \text{where} \quad \tilde{\sigma}_\beta = \frac{\beta^L - \beta^R}{\alpha(\beta^L) - \alpha(\beta^R)}.$$

Note that relation between the graphs of $\mathcal{F}^L$ and $\mathcal{F}^R$ are topologically identical to that of the graphs of F^L and F^R. Riemann problem for a scalar conservation law with (F^L, F^R) as the flux function, will generate the same types of waves if using $(\mathcal{F}^L, \mathcal{F}^R)$ as the flux functions, although with different wave speeds. The advantage of using $\mathcal{F}^L$ and $\mathcal{F}^R$ lies in the fact that β-waves will be stationary. This makes the construction of Riemann solution clearer. For the Riemann data (4.6), we are now consider the following scalar equation

$$(4.8) \qquad C_t + \mathcal{F}(C, x)_x = 0, \qquad \text{where} \qquad \mathcal{F}(C, x) = \begin{cases} \mathcal{F}^L(C), & x \leq 0, \\ \mathcal{F}^R(C), & x > 0. \end{cases}$$

Existence and uniqueness of Riemann solution for scalar conservation law with flux function with spacial discontinuity was established by Gimse & Risebro [9], using the minimum jump condition, under the assumption that the flux functions $f(u, x)$ are smooth in u. Our flux functions $\mathcal{F}(C, x)$ are only continuous and piecewise smooth in C. Nevertheless, the construction of the Riemann solution remains rather similar.

We denote $(u^1, u^2; f)$ the Riemann problem for a scalar conservation law $u_t + f(u)_x = 0$ with u^1, u^2 as the left and right states. The construction follows a three-step algorithm.

S1: Given $\mathcal{F}^L(C)$ and C^L, we identify the set

$$I^L(C^L, \mathcal{F}^L) \doteq \left\{ C^m; \ (C^L, C^m; \mathcal{F}^L) \text{ is solved by waves of non-positive speed} \right\} \cup \{C^L\}.$$

S2: Given $\mathcal{F}^R(C)$ and C^R, we identify the set

$$I^R(C^R, \mathcal{F}^R) \doteq \left\{ C^M; \ (C^M, C^R; \mathcal{F}^R) \text{ is solved by waves of non-negative speed} \right\} \cup \{C^R\}.$$

S3: Find the β-wave position (C^m, β^L)-(C^M, β^R) by

$$\text{minimizing} \left| C^M - C^m \right| \text{ in the set} \quad \left\{ C^m \in I^L, C^M \in I^R, \mathcal{F}^L(C^m) = \mathcal{F}^R(C^M) \right\}.$$

Next Theorem guarantees the existence and uniqueness of the Riemann solution.

Theorem 4.1. *Consider the Riemann problem with $u^L = (C^L, \beta^L)$ and $u^R = (C^R, \beta^R)$ as the left and right states, where β^L and β^R is connected with a single β shock. There exists a unique solution for this Riemann problem.*

Proof. We first observed that it suffices to prove the existence and uniqueness of the path for the β-shock. Once this path is located, the solution for the Riemann problem is uniquely determined. We define the set for the values of the flux function on the set I^L and I^R as

$$(4.9) \qquad J^L(C^L, \mathcal{F}^L) \doteq \left\{ \mathcal{F}^L(C); C \in I^L \right\}, \qquad J^R(C^R, \mathcal{F}^R) \doteq \left\{ \mathcal{F}^R(C); C \in I^R \right\}.$$

We first claim that the intersection of these two sets are not empty,

$$(4.10) \qquad\qquad\qquad J^L(C^L, \mathcal{F}^L) \cap J^R(C^R, \mathcal{F}^R) \neq \emptyset.$$

Indeed, due to the properties of our flux function, it is convenient to list all the cases. Given $\mathcal{F}^L$, let $(C_0, \mathcal{F}_0^L)$ and $(C_2, \mathcal{F}_2^L)$ be the minimum and maximum points, respectively. Also we let C_1 be the unique point such that $C_0 < C_1 < C_2$ and $\mathcal{F}^L(C_1) = 1$. See Figure 6 for an illustration. There are 4 cases.
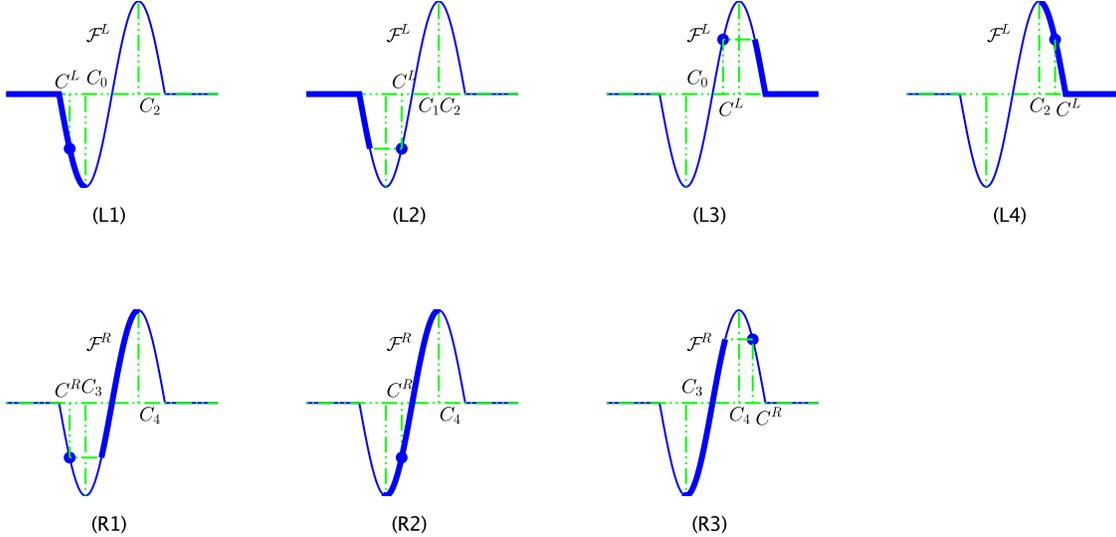
Figure 6: The set I^L and J^L are the x and y coordinates for the thick curves in (L1)-(L4). The set I^R and J^R are the x and y coordinates for the thick curves in (R1)-(R3).

- If $C^L \leq C_0$, then we have

$$I^L = (0, C_0], \qquad J^L = [\mathcal{F}^L(C_0), 1].$$

13

- If $C_0 < C^L < C_1$, then let $\tilde{C}_L$ be the unique point such that $\tilde{C}_L < C_0$ and $\mathcal{F}^L(\tilde{C}_L) = \mathcal{F}^L(C^L)$. We have

$$I^L = (-\infty, \tilde{C}_L] \cup \{C^L\}, \qquad J^L = [\mathcal{F}^L(C^L), 1].$$

- If $C_1 < C^L < C_2$, then let $\tilde{C}_L$ be the unique point such that $\tilde{C}_L > C_2$ and $\mathcal{F}^L(\tilde{C}_L) = \mathcal{F}^L(C^L)$. We have

$$I^L = \{C^L\} \cup [\tilde{C}_L, 1), \qquad J^L = [1, \mathcal{F}^L(C^L)].$$

- If $C^L \geq C_2$, then we have

$$I^L = [C_2, 1), \qquad J^L = [1, \mathcal{F}^L(C_2)].$$

We note that $1 \in J^L$ in all cases.

Now, given $\mathcal{F}^R$, let $(C_3, \mathcal{F}_3^R)$ and $(C_4, \mathcal{F}_4^R)$ be the minimum and maximum points for $\mathcal{F}^R$ respectively. There are 3 cases, illustrated in Figure 6.

- If $C^R < C_3$, then let $\tilde{C}_R$ be the unique point such that $\tilde{C}_R > C_3$ and $\mathcal{F}^R(\tilde{C}_R) = \mathcal{F}^R(C^R)$. We have
$$I^R = \{C^R\} \cup [\tilde{C}_R, C_4], \qquad J^R = [\mathcal{F}^R(\tilde{C}_R), \mathcal{F}_4^R].$$
This includes the case where C^R lies in the single phase region on the left of D_2.

- If $C_3 \leq C^R \leq C_4$, then we have

$$I^R = [C_3, C_4], \qquad J^R = [\mathcal{F}_3^R, \mathcal{F}_4^R].$$

- If $C^R > C_4$, then let $\tilde{C}_R$ be the unique point such that $\tilde{C}_R < C_4$ and $\mathcal{F}^R(\tilde{C}_R) = \mathcal{F}^R(C^R)$. We have
$$I^R = [C_3, \tilde{C}_R] \cup \{C^R\}, \qquad J^R = [\mathcal{F}_3^R, \mathcal{F}^R(\tilde{C}_R)].$$
This includes the case where C^R lies in the one phase region on the right of D_2.

We note that $1 \in J^R$. Thus $J^L \cap J^R$ is non-empty, proving (4.10).

To see that there is a unique solution to the minimizing problem, we first exclude the possible isolated points in the sets I^L, I^R, and denote the sets by I_o^L, I_o^R. On the set I_o^L, the function $\mathcal{F}^L(C)$ is strictly decreasing, while on the set I_o^R, the function $\mathcal{F}^R(C)$ is strictly increasing. Given $\mathcal{F} \in J^L \cap J^R$, let $C^M \in I^R$ and $\mathcal{F}^R(C^M) = \mathcal{F}$, and let $C^m \in I^L$ and $\mathcal{F}^L(C^m) = \mathcal{F}$. Denote also $D_{\mathcal{F}} \doteq C^M - C^m$. Then, the function $\mathcal{F} \mapsto D_{\mathcal{F}}$ is strictly increasing, and there exits a unique minimum for the map $\mathcal{F} \mapsto |D_{\mathcal{F}}|$.

Finally, if $\mathcal{F}^L(C^L)$ and/or $\mathcal{F}^R(C^R)$ are/is in $J^L \cap J^R$, there could be multiple minimum paths. In this case, we will select the path with the more isolated points. This yields a unique path for the β-shock. $\qquad \square$

14

We have an immediate Corollary on the location of the β-shock.

Corollary 4.2. *In the setting of Theorem 4.1, the path of the β-shock lies on the same side of EVC as the left state of the Riemann data.*

Sample Riemann problems connecting single phase and two-phase regions. Let l_t be the tie-line that is tangent to the two-phase region, and let (C_t, β_t) be the tangent point. This tie-line lies in the single phase region, and the the flux function $F(C, \beta_t) = C$. Consider another tie-line l_2 through the two-phase region with the flux $F(C, \beta_2)$. The solutions for the Riemann problems with left and right states on each of these tie-lines are illustrated in Figure 7, where we plotted the functions $F(C, \cdot)$.

Case 1. If the left state is l_t, then it will be connected to the point M with a C-contact discontinuity that travels with speed 1. Note that M is on the EVC. In fact it is the endpoint of EVC as it reaches the single-phase region. From M one can connect to any R on the tie-line l_2 on the red curve by solving a Riemann problem of a scalar equation, which will yield a shock of speed ≥ 0.

Case 2. (a) If the right state is on l_t, and the left state is on the the right side of the EVC on the tie-line l_2, then the wave path L-M-R will go through the upper point for M. (b) On the other hand, if the left state is on the left of the EVC on the tie-line l_2, the wave path L-M-R will go through the lower point for M.
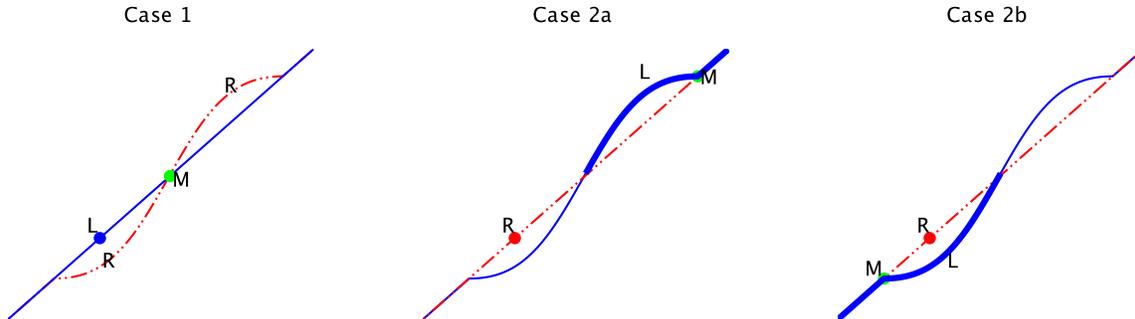
Figure 7: Riemann solver for the special case, where a tie-line is tangent to the two phase region, plots of the functions $C \mapsto F(\cdot, \beta^L)$ and $C \mapsto F(\cdot, \beta^R)$, where blue curve is for the left state, and red curve is for the right state.

Finally, if the left or right state are in the single-phase region along a tie-line extension, the single-phase region and two-phase region is connected by a C-wave [**?**].

These discussions indicate that there are two ways that a wave path can connect states in the single-phase and two-phase regions: (i) through tie lines, and (ii) through the point M in Case 1. This point M is referred to as the *Plait Point*.

15

4.2 Connecting β-rarefaction wave to C-waves

Definition 4.3. *In the (C, β)-plane, given a β-integral curve C, a curve $\widehat{C}$ is called the* critical curve *of C, if for every fixed β the β-eigenvalue*

$$\lambda^\beta(C, \beta) = \mathcal{F}(C; \beta, \alpha'(\beta)^{-1})$$

has the same values on the curves C and $\widehat{C}$, and the curves C and $\widehat{C}$ are separated by the degenerate curve.

Due to the S-shape of the flux function $C \mapsto F$, the existence and uniqueness of the critical curve is clear. Next Lemma provides its relative location to the β-integral curves.

Lemma 4.4. *Let $C_1 \cup C_2$ be a β-integral curve, separated by the degenerate curve with C_1 on the left and C_2 on the right, lying on the same side of EVC. Let C_3 and C_4 be the corresponding critical curves for C_1 and C_2 respectively. Then, either C_3 is on the left of C_2 and C_4 is on the left of C_1, or C_3 is on the right of C_2 and C_4 is on the right of C_1.*

Proof. We parametrize all these curve with β, i.e., C_1 is the graph of the function $\beta \mapsto C_1(\beta)$ etc. We first observe that

$$\lambda^\beta(C_1, \beta) = \frac{F(C_1, \beta)\alpha' + 1}{C_1\alpha' + 1} = \frac{F(C_3, \beta)\alpha' + 1}{C_3\alpha' + 1} = \lambda^\beta(C_3, \beta)$$

implies

$$(4.11) \qquad \frac{F(C_1, \beta) - C_1}{F(C_3, \beta) - C_3} = \frac{F(C_1, \beta)\alpha' + 1}{F(C_3, \beta)\alpha' + 1} = \frac{C_1\alpha' + 1}{C_3\alpha' + 1}.$$

Along C_1, using (2.6), the directional derivative of the β-eigenvalue is

$$(4.12) \qquad \nabla\lambda^\beta \cdot r^\beta = \frac{\alpha''(\beta)(F(C_1, \beta) - C_1)}{(\alpha'(\beta) + 1)^2}.$$

Along C_3, the directional derivative of the β-eigenvalue is the same as in (4.12). We must have

$$(4.13) \qquad \lambda_C^\beta(C_3, \beta)C_3'(\beta) + \lambda_\beta^\beta(C_3, \beta) = \frac{\alpha''(\beta)(F(C_1, \beta) - C_1)}{(C_1\alpha'(\beta) + 1)^2}.$$

Note that $\lambda^\beta(C_1, \beta) = \lambda^\beta(C_3, \beta)$, and we will simply write λ^β. Also, since $\alpha(\beta)$ is a function of β, we will drop the independent variable and simply write $\alpha, \alpha', \alpha''$.

Using the partial derivatives

$$\lambda_C^\beta = \frac{(F_c - \lambda^\beta)\alpha'}{C\alpha' + 1}, \qquad \lambda_\beta^\beta = \frac{F_\beta\alpha' + F\alpha'' - \lambda^\beta C\alpha''}{C\alpha' + 1},$$

and the identities (4.11), we can solve (4.13) with respect to C_3' and obtain

$$
\begin{aligned}
C_3'(\beta) &= \frac{1}{(F_C(C_3, \beta) - \lambda^\beta)\alpha'} \left[\frac{(C_3\alpha' + 1)^2}{(C_1\alpha' + 1)^2} \cdot \frac{\alpha''(F(C_1, \beta) - C_1)}{(C_3\alpha' + 1)} \right. \\
&\qquad\qquad \left. - F_\beta(C_3, \beta)\alpha' - F(C_3, \beta)\alpha'' + \lambda^\beta C_3\alpha'' \right] \\
&= \frac{1}{(F_C(C_3, \beta) - \lambda^\beta)\alpha'} \left[\frac{(F(C_3, \beta) - C_3)\alpha''}{C_1\alpha' + 1} - F_\beta(C_3, \beta)\alpha' - (F(C_3, \beta) - \lambda^\beta C_3)\alpha'' \right].
\end{aligned}
$$

16

Fix a point on C_3, denoted as (C_3, β), let C_5 denote the β-integral curve through (C_3, β), parametrize it in β. We have

$$C_5'(\beta) = -\frac{F_\beta(C_3, \beta)}{F_C(C_3, \beta) - \lambda^\beta}.$$

Direct computation gives

$$
\begin{aligned}
C_3'(\beta) - C_5'(\beta) &= \frac{\alpha''}{(F_C(C_3, \beta) - \lambda^\beta)\alpha'} \left[\frac{F(C_3, \beta) - C_3}{C_1\alpha' + 1} - F(C_3, \beta) + \lambda^\beta C_3 \right] \\
&= \frac{\alpha''}{(F_C(C_3, \beta) - \lambda^\beta)\alpha'} \left[\frac{F(C_3, \beta) - C_3}{C_1\alpha' + 1} - F(C_3, \beta) + \frac{F(C_1, \beta)\alpha' + 1}{C_1\alpha' + 1} C_3 \right] \\
&= \frac{\alpha''}{F_C(C_3, \beta) - \lambda^\beta} \left[F(C_1, \beta)C_3 - F(C_3, \beta)C_1 \right] \\
&= \frac{\alpha'' C_1 C_3}{F_C(C_3, \beta) - \lambda^\beta} \left[\frac{F(C_1, \beta)}{C_1} - \frac{F(C_3, \beta)}{C_3} \right].
\end{aligned}
$$

The factor $F_C(C_3, \beta) - \lambda^\beta$ changes sign crossing the degenerate curves, and the term $F(C_1, \beta)/C_1 - F(C_3, \beta)/C_3$ changes from positive to negative as it crosses EVC. We always have $C_1 \geq 0, C_2 \geq 0$. We have the following conclusion:

Case 1. If $\alpha'' < 0$, then on the left of EVC, we have

$$F_C(C_3, \beta) - \lambda^\beta > 0, \quad F(C_1, \beta)/C_1 - F(C_3, \beta)/C_3 < 0, \qquad \rightarrow \qquad C_3' > C_5'.$$

By the uniqueness of the β-integral curve, C_3 lies on the right of C_2. Similarly, C_4 lies on the right of C_1.

If these curves lie on the right of EVC, then we have

$$F_C(C_3, \beta) - \lambda^\beta < 0, \quad F(C_1, \beta)/C_1 - F(C_3, \beta)/C_3 > 0, \qquad \rightarrow \qquad C_3' > C_5'.$$

Then, C_3 lies on the right of C_2, and similarly C_4 lies on the right of C_1.

Case 2. If $\alpha'' > 0$, a completely similar argument shows that C_3 lies on the left of C_2, and C_4 lies on the left of C_1.

These two cases are illustrated in Figure 8, on the left of EVC. $\qquad \square$

Next Theorem establishes the existence and uniqueness of solutions for a Riemann problem which contains β-rarefaction waves.

Theorem 4.5. *Consider the Riemann problem with $u^L = (C^L, \beta^L)$ and $u^R = (C^R, \beta^R)$ as the left and right state, where β^L and β^R is connected with a single β rarefaction wave. There exists a unique solution for this Riemann problem.*

Proof. Under our assumptions, given β^L and β^R, then either (i) every point on $\beta = \beta^R$ can be connected to β^L through a β-integral curve, or (ii) every point on $\beta = \beta^L$ can be connected to β^R through a β-integral curve. To fix the idea, we consider case (i), while case (ii) can be treated in a completely similar way.

17
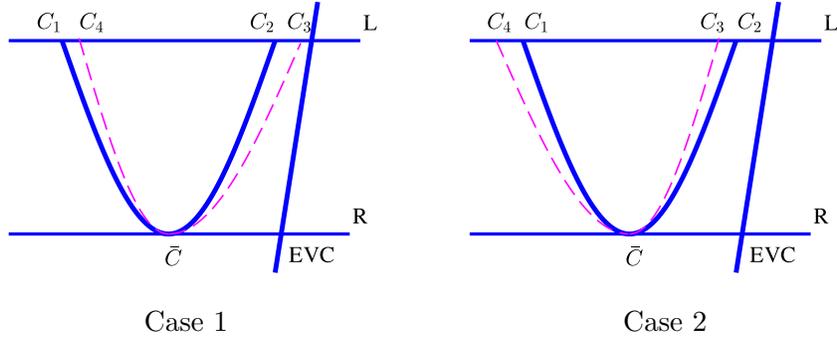
Figure 8: Two possible relations between the curves C_1, C_2, C_3 and C_4.

Recall the definition of the function $\mathcal{F}(C; \beta, a)$ in (2.7). We denote now

$$\mathcal{F}^L(C) = \mathcal{F}(C; \beta^L, \alpha'(\beta^L)^{-1}), \qquad \mathcal{F}^R(C) = \mathcal{F}(C; \beta^R, \alpha'(\beta^R)^{-1}).$$

Let $\bar{C}, \hat{C}$ be the two values where $\mathcal{F}^R$ reaches its min and max value. Then, there exists two integral curves through each of $\bar{C}$ and $\hat{C}$ that connect to β^L. We denote these curves as $C_1, C_2, \tilde{C}_1, \tilde{C}_2$.

On the line $\beta = \beta^L$, we denote by I' the set of C values that can not be connected to the right with a β-integral curve. Clearly, this set includes the C values between the curves C_1 and C_2, and those between the curves $\tilde{C}_1$ and $\tilde{C}_2$.

Given u^L, we let $\tilde{I}^L$ denote the set of C values on the line $\beta = \beta^L$ such that the Riemann problem $(C^L, C; F^L)$ is solved with non-positive speed, and the point C can be connected to $\beta = \beta^R$ along a β-integral curve. Recall the sets I^L and I^R used in the proof of Theorem 4.1. We have

$$\tilde{I}^L = I^L \setminus I'.$$

Furthermore, let $\hat{I}^L$ denote the set of the corresponding C values on the line $\beta = \beta^R$ that can be connected to the set $\tilde{I}^L$ through a β-rarefaction curve.

We will only consider the case where the β-rarefaction path lies on the left of the EVC, while the other case can be treated similarly. We consider the two Cases in Figure 8 separately.

Case 1. We assume first that C^L lies on the left side of EVC, and we identify the set $\hat{I}^L$ for all cases of C^L locations. In Figure 9 we show three different situations.

- If $C^L < C_2$, then $\tilde{I}^L$ contains the interval on the left of C_1 and $\hat{I}^L$ contains the interval on the left of $\bar{C}$. The set $\hat{I}^L \cap I^R$ includes exactly one point.

- If $C_2 < C^L < C_3$, then $\tilde{I}^L$ contains an addition point C^L, and $\hat{I}^L$ contains an additional point which can be connected to C^L through a β-integral curve. The set $\hat{I}^L \cap I^R$ includes either one point or two points. If it includes two points, one of then must be the isolated point in $\hat{I}^L$, which will be selected.

- If $C_3 < C^L < C_0$, we denote the integral curve through C^L by C_4 and it corresponding critical curve by C_5. Then the set $\tilde{I}^L$ includes the point C^L plus the interval on the left of the critical curve C_5. The set $\hat{I}^L$ consists of the point on C_4 and the interval on

18
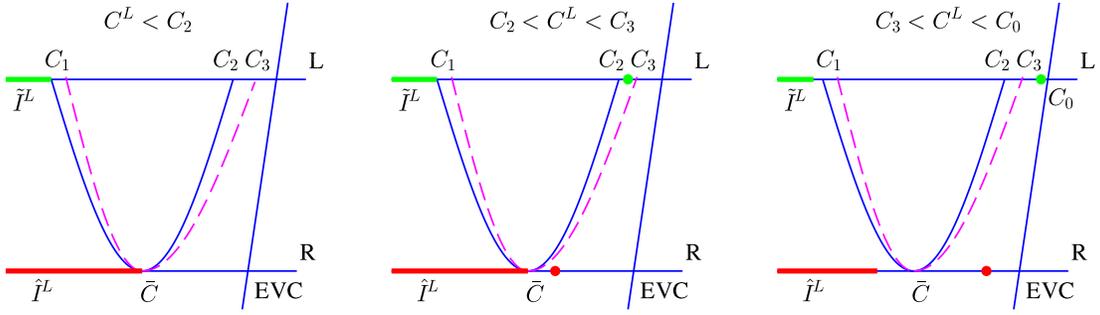
Figure 9: Three situations for different locations of C^L and the corresponding sets of $\tilde{I}^L$ (with thick three line on L) and $\hat{I}^L$ (with thick red line on R).

the left of the point that can be connected to $\tilde{I}^L$ with integral curve, where the right endpoint lies on the left of C_5. Thus, the set $\hat{I}^L \cap I^R$ includes exactly one point.

Case 2. The proof is very similar, except in the case when $C_3 < C^L < C_2$, where there exists composite pathes, see Figure 10. In the plot on the left, C^L can be connected to $\bar{C}$ as follows: From C^L, the path follows a β-integral curve, until it intersects with the critical curve C_3 at a. Then it takes a horizontal path, through a C-shock, until it reaches the curve C_1 at b. From there it follows C_1 to reach $\bar{C}$. In the plot on the right, we show another path. In fact, at any point $\bar{a}$ before reaching a, one could take a horizontal path to reach the critical curve of the integral curve through C^L at $\bar{b}$, then take the β-integral curve from there to reach the line $\beta = \beta^R$ at a point to the left of $\bar{C}$. Thus, we redefine the set $\hat{I}^L$ to include the points on the line $\beta = \beta^R$ that can be connected to the set $\tilde{I}^L$ through a composite path. Clearly, $\hat{I}^L$ includes all $C \le \hat{C}$. Following a same argument as for Case 1, we conclude the uniqueness of the path. □
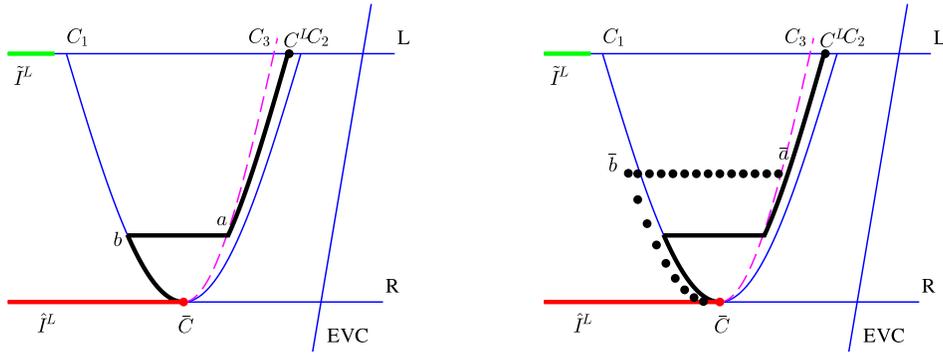
Figure 10: Case 2, when $C_3 < C^L < C_2$, the β-wave path consists of two β-rarefaction waves with a C-contact in between.

Similar to Corollary 4.2, we immediately have the next result on the position of the β-rarefaction wave.

Corollary 4.6. *In the setting of Theorem 4.5, the path of the β-rarefaction lies on the same side of the EVC as the left state u^L.*

4.3 Global existence and uniqueness of solutions for Riemann problems

Proof. (Of Theorem 2.1.) We now complete a constructive proof for the main Theorem. Given a left and right state $u^L = (C^L, \beta^L)$ and $u^R = (C^R, \beta^R)$, the solution of the Riemann problem is constructed in two steps. We first solve the β-wave using information beaded on (β^L, β^R) and the equation (1.11). This determines the type of β-wave that will connect to the possible C-waves on the left and right. Thanks to Theorem 4.1 and Theorem 4.5, there exists a unique path for the location of the β-wave. Then, the C-waves are constructed by solving the scalar conservation laws, possibly for both left and right equations with $\beta = \beta^L$ and $\beta = \beta^R$. The uniqueness of these C-waves follows from standard theory for scalar conservation laws. Thus, combining with Corollary 4.2 and Corollary 4.8 we complete the proof of Theorem 2.1. $\square$

We have two immediate Corollaries.

Corollary 4.7. *The two-phase region is invariant for Riemann problems. Furthermore, the EVC cuts the region into two sub-regions, where each one is invariant for Riemann problems.*

For example, if both u^L and u^R lie on the left (or on the right) of the EVC with $F^L \geq C^L$ and $F^R \geq C^R$, then the solution remains on the same side of the EVC and $F \geq C$.

Combining Corollary 4.7 and Corollary 4.6, the next Corollary follows.

Corollary 4.8. *Let $u^L = (C^L, \beta^L)$ and $u^R = (C^R, \beta^R)$ be the left and right states of the Riemann problem, where (β^L, β^R) is connected with a single β-wave, i.e., either a β-shock or a β-rarefaction wave. Then, the path of β-wave wave and the left state lie on the same side of the EVC. Furthermore, the solution path in the phase plane (C, β) crosses the EVC exactly once.*

5 Numerical Simulations with Front Tracking

The Riemann solver as described in section 4.3 is implemented in a front tracking algorithm. The results of the front tracking is demonstrated for several examples and are compared with finite difference simulation results.

Let $\varepsilon > 0$ be the parameter for the front tracking algorithm. We discretize the space for β values, and let $\mathcal{B}^\varepsilon = \{\beta^n\}$ denote the set of the discrete values for β, with

$$(5.1) \qquad \beta^n > \beta^{n-1}, \qquad \left|\beta^n - \beta^{n-1}\right| \leq \varepsilon, \qquad n = 1, 2, \cdots, N-1.$$

We let $\alpha^\varepsilon(\beta)$ denote the piecewise affine approximation to $\alpha(\beta)$, with $\alpha^\varepsilon(\beta^n) = \alpha(\beta^n)$ for every n.

Next, we need to discretize C along each tie line. Unfortunately, the C grid is not constant and depend on the β-wave. Therefore, we need to update the $\mathcal{C}^\varepsilon = \{C^{n,m}\}$ after calculating a new β-wave. The set of $\mathcal{C}^\varepsilon = \{C^{n,m}\}$ denote the discritized values for C, with

$$(5.2)$$
$$C^{n,m} > C^{n,m-1}, \qquad \left|C^{n,m} - C^{n,m-1}\right| \leq \varepsilon^C, \qquad n = 1, 2, \cdots, N-1, \qquad m = 1, 2, \cdots, M-1.$$

Then we estimate $f(S)$ with piecewise linear $f^\varepsilon(S)$. The parameter ε^C is ε devided by a constant.

The discrete initial data is piecewise constant $u^\varepsilon(0, x) = (C^\varepsilon(0, x), \beta^\varepsilon(0, x))$, where β^ε takes only the values in $\mathcal{B}^\varepsilon$. Let x_i be the points of discontinuities in the discrete initial data. We denote the cell values as

$$\beta^\varepsilon(0, x) = \beta_i, \quad C^\varepsilon(0, x) = C_i, \qquad x_{i-1} \le x < x_i.$$

At $t = 0$, a set of Riemann problems shall be solved at every point x_i where the initial discrete data has a jump. The rarefaction fronts are approximated by jumps of size less than or equal to ε (Figure 11, Left). One can use the result of the Theorem 4.5 to calculate the intermediate points, where both approaches result to the same solution (Figure 11, right). Each front is labeled to be either C-front or β-front, and it travels with Rankine-Hugonoit velocity. At a later time $t > 0$ where two fronts meet, a new Riemann problem is solved. The process continues until the final time T is reached. In case of variation of injection condition, the initialization process should be repeated.

The β and C values calculated by front tracking has a significant different behavior. The definition of $\alpha^\varepsilon(\beta^n)$ constrains the values of β in the solution to $\mathcal{B}^\varepsilon$, unless the initial data contain values out of $\mathcal{B}^\varepsilon$. However the C values of solution are not necessarily in $\mathcal{C}^\varepsilon$ even if all the initial data are in $\mathcal{C}^\varepsilon$. Therefore, to control the number of fronts, C-waves with the same velocity should be merged into one C-wave, and C-waves smaller than a threshold should be eliminated.

We used a three component system with properties shown in tables 1 and 2 at 2650 $psia$ and 160°F. Peng–Robinson equation of state [31] is used to calculate phase compositions.

	$T_C(°\text{F})$	$P_c(psi)$	ω
C_{10}	611.161	305.76	0.5764
CO_2	87.89	1071	0.225
C_1	-116.59	667.8	0.008

Table 1: Fluid characterization for the ternary system

	CO_2	C_1
C_{10}	0.0942	0.0420
CO_2	-	0.1

Table 2: Binary interaction coefficients for the ternary system

Slug injection is commonly used in gas flooding where the boundary condition at $x = 0$ is changed at different times (or cycles). Furthermore, the finite difference simulation with single–point upwind flux estimation is used to simulate gas flooding. We compared the simulation results of the front tracking algorithm with the finite difference simulations. Example 2 has initial oil shown by R in Figure 12 and slug composition by L_1, which changes to L_2 at $t = 0.2$. Figure 12 compares the compositions at $t = 0.8$ and figure 13 shows the comparison of composition profiles at $t = 0.8$.

Example 3 is simulation of a problem with variable initial condition. In addition, the composition at $x = 0$ is varied at different times to mimic the slug injection process. Figure 14 shows the fronts of the example, and Figure 15 shows the profiles at different times.
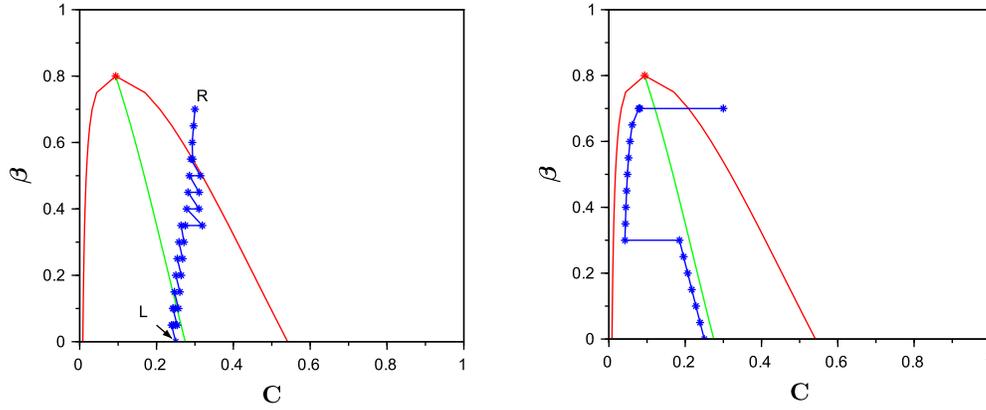
Figure 11: Estimation of large β-rarefaction with smaller waves (Left) and convergence of results to the correct solution (Right)
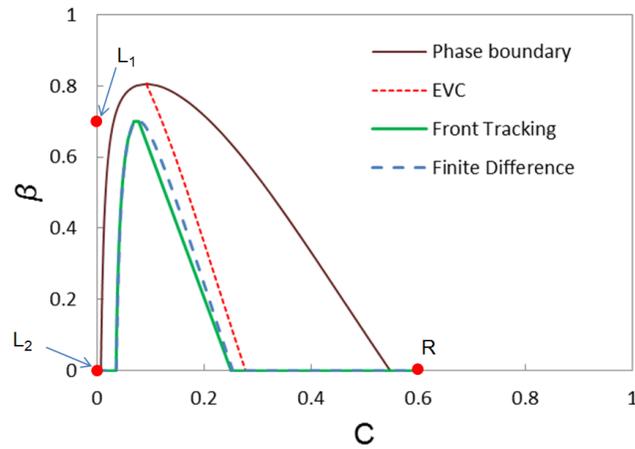
Figure 12: Comparison of the composition path calculated by finite difference simulation and front tracking
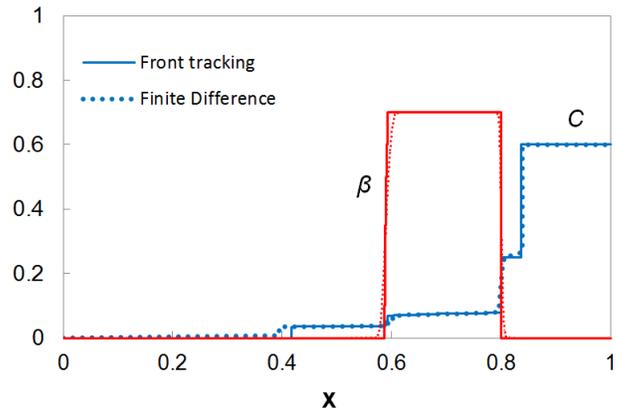
Figure 13: Comparison of the composition profiles calculated by finite difference simulation using 10,000 grid blocks and front tracking with $\varepsilon = 0.05$
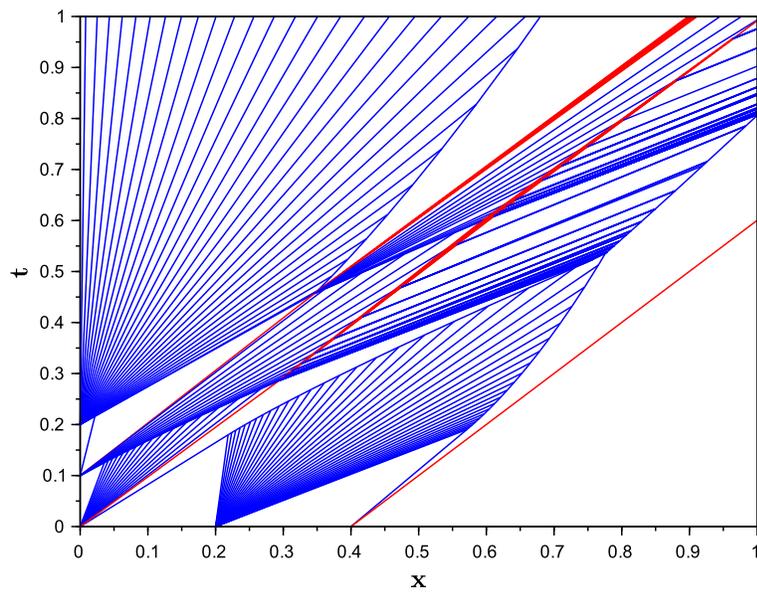
Figure 14: Fronts for variation of initial condition where two slugs are injected.
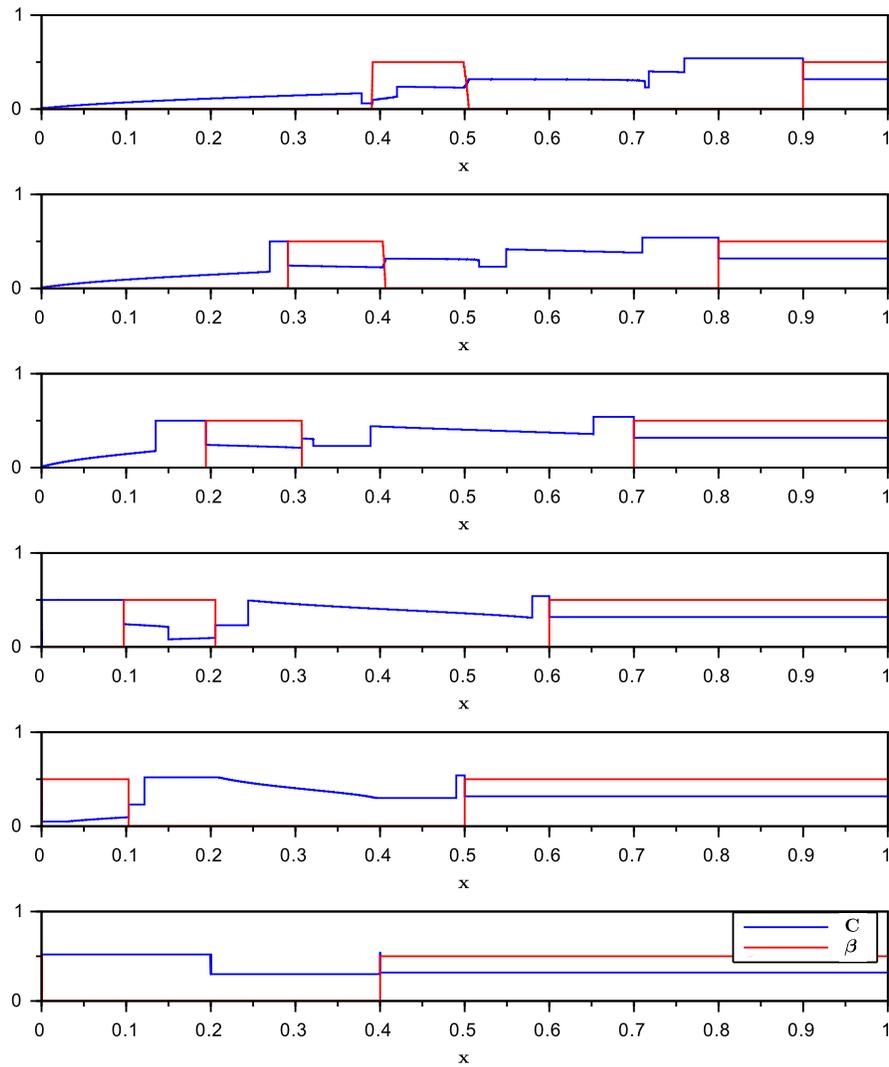
Figure 15: Composition profiles at $t = 0.0$ (bottom), $0.1, 0.2, 0.3, 0.4$ and 0.5 (top)

$< x$	$x <$	C	β
0	0.2	0.52	0
0.2	0.4	0.3	0
0.4	inf	0.318	0.5

Table 3: Initial condition for example problem 3

$< t$	$t <$	C	β
0	0.1	0.05	0.5
0.1	0.2	0.5	0
0.2	inf	0.01	0

Table 4: Injection condition for example problem 3

6   Concluding remarks

Through a constructive proof, we show the existence and uniqueness for solution of global Riemann problem for a two phase flow model with three-component gas flooding in reservoir simulation. The construction of Riemann solution offers a front tracking algorithm, allowing numerical simulations for case studies.

A more interesting and challenging problem is the existence of entropy weak solutions for the Cauchy problem, established as the convergence limit of the front tracking approximate solutions. Towards this goal, one needs to establish proper a-priori estimates on the approximate solutions, in particular, some bounds on the total variation in certain form for compactness. The key step in these analysis is the wave interaction estimates. In the literature among models on reservoir simulation, the existence of entropy weak solutions is only available for non-adsorptive models for two phase polymer flooding, under specific assumptions. For our problem, due to the various degeneracies and the nonlinear resonance, this remains an open problem.

References

[1] K. Ahmadi, R.T. Johns, K. Mogensen, R. Noman, Limitations of current method-of-characteristics (MOC) methods using shock-jump approximations to predict MMPs for complex gas/oil displacements. *SPE J.,* **16** (2011), 743–750.

[2] S. Bianchini, A. Bressan, Vanishing viscosity solutions of nonlinear hyperbolic systems, *Ann. of Math.* **161** (2005), 223–342.

[3] A. Bressan, *Hyperbolic Systems of Conservation Laws. The One Dimensional Cauchy Problem.* Oxford University Press, 2000.

[4] S.E. Buckley, M. Leverett, Mechanism of fluid displacement in sands. *Transactions of the AIME,* **146** (1942), 107–116.

[5] O. Dahl, T. Johansen, A. Tveito, R. Winther, Multicomponent chromatography in a two phase environment. *SIAM J. Appl. Math.* **52** (1992), 65–104.

[6] B. Dindoruk, Analytical theory of multiphase multicomponent displacement in porous media. *Doctoral dissertation, Stanford University,* (1992).

[7] A.M. Egwuenu, R.T. Johns, Y. Li, Improved fluid characterization for miscible gas floods. *SPERE,* **11** (2008), 655–665.

[8] V.M. Entov, A. Zazovsky, Nonlinear waves in physicochemical hydrodynamics of enhanced oil recovery. Multicomponent flows. *International Conference on Porous Media: Physics, Models, Simulation,* Moscow (1997).

[9] T. Gimse, N.H. Risebro, Riemann problems with a discontinuous flux function. In *Proc. Third Internat. Conf. on Hyperbolic Problems. Theory, Numerical Method and Applications.* (B. Engquist, B. Gustafsson. eds.) Studentlitteratur/Chartwell-Bratt, Lund-Bromley, (1991), 488-502.

[10] T. Gimse, N.H. Risebro, Solution of the Cauchy problem for a conservation law with discontinuous flux function. *SIAM J. Math. Anal.* **23** (1992), 635–648.

[11] F.G. Helfferich, Theory of multicomponent, multiphase displacement in porous media. *SPEJ* **21** (1980), 51–62.

[12] G.J. Hirasaki, Application of the theory of multicomponent, multiphase displacement to three-component, two-phase surfactant flooding, *SPEJ* **21** (1981), 191–204.

[13] E. Isaacson, B. Temple, Analysis of a singular hyperbolic system of conservation laws. *J.Differential Equations,* **65** (1986), pp. 250–268.

[14] T. Johansen, A. Tveito, R. Winther, A Riemann solver for a two-phase multicomponent process. *SIAM J. Sci. Statist. Comput.* **10** (1989), 846–879.

[15] T. Johansen, R. Winther, The solution of the Riemann problem for a hyperbolic system of conservation laws modelling polymer flooding. *SIAM J. Math. Anal.,* **19** (1988), pp. 541–566.

[16] T. Johansen, R. Winther, Mathematical and numerical analysis of a hyperbolic system modeling solvent flooding. *ECMOR II – 2nd European Conference on the Mathematics of Oil Recovery,* (1990).

[17] T. Johansen, R. Winther, Mathematical and numerical analysis of a hyperbolic system modeling solvent flooding. *SIAM J. Math. Anal.,* **20** (1989), 908–929.

[18] R.T. Johns, Analytical theory of multicomponent gas drives with two-phase mass transfer. *Doctoral dissertation, Stanford University,* (1992).

[19] R.T. Johns, B. Dindoruk, F.M. Orr, Analytical theory of combined condensing/vaporizing gas drives. *SPE Adv. Tech. Series,* **1** (1993), 7–16.

[20] R.T. Johns, F.M., Orr, Miscible gas displacement of multicomponent oils. *SPE J.,* **1** (1996), 39–50.

[21] R. Juanes, K.A. Lie, Numerical modeling of multiphase first-contact miscible flows. Part 2. Front-tracking/streamline simulation. *Transport in Porous Media,* **72** (2008), 97–120.

[22] B. Keyfitz, H. Kranzer, Asystem of non-strictly hyperbolic conservation laws arising in elasticity theory, *Arch. Rational Mech. Anal.,* **72** (1980), 219-241.

[23] S. Khorsandi, K. Ahmadi, R.T. Johns, Analytical solutions for gas displacements with bifurcating phase behavior. *SPE J.,* **19** (2014), 943–955.

[24] S. Kruzhkov, First-order quasilinear equations with several space variables. *Math. USSR Sb.* **10** (1970), 217–273.

[25] T.C. LaForce, R.T. Johns Effect of Quasi-Piston-Like Flow on Miscible Gasflood Recovery. *SPE Western Regional Meeting* (2005).

[26] K.A. Lie, R. Juanes, A front-tracking method for the simulation of three-phase flow in porous media. *Computational Geosciences,* **9** (2005), 29–59.

[27] P.D. Lax, Hyperbolic systems of conservation laws II. *Comm. Pure Appl. Math.* **10** (1957), 537–566.

[28] T.P. Liu, The entropy condition and the admissibility of shocks. *Journal of Mathematical Analysis and Applications* **53** (1976), 78–88.

[29] M. Michelsen, The isothermal flash problem. Part II. Phase-split calculation. *Fluid Phase Equilibr.* **9** (1982), 21–40.

[30] F.M. Orr, R.T. Johns, B. Dindoruk, Development of miscibility in four-component CO2 floods. *SPERE*, **8** (1993), 135–142.

[31] D.Y. Peng, D.B. Robinson, A new two-constant equation of state. *Industrial & Engineering Chemistry Fundamentals* **15** (1976), 59–64.

[32] A.P. Pires, P.G. Bedrikovetsky, A.A. Shapiro, A splitting technique for analytical modelling of two-phase multicomponent flow in porous media. *Journal of Petroleum Science and Engineering* **51** (2006), 54–67.

[33] G.A. Pope, The application of fractional flow theory to enhanced oil recovery. *SPEJ* **20** (1980), 191–205.

[34] H-K. Rhee, R. Aris, N.R. Amundson, On the theory of multicomponent chromatography, *Philos. Trans. Roy. Soc.,* London Ser. A, **267** (1970), 419–455.

[35] C.J. Seto, F.M. Orr, Analytical solutions for multicomponent, two-phase flow in porous media with double contact discontinuities. *Transport in Porous Media* **78** (2008), 161–183.

[36] J.A. Smoller, On the solution of the Riemann problem with general step data for an extended class of hyperbolic systems. *The Michigan Mathematical Journal* **16** (1969), 201–210.

[37] B. Temple, Systems of conservation laws with invariant submanifolds, *Trans. Amer. Math. Soc.*, **280** (1983), 781–794.

[38] D. Wagner, Equivalence of the Euler and Lagrangian equations of gas dynamics for weak solutions. *J. Differential Equations*, **68** (1987), 118–136.

[39] Y. Wang, F.M. Orr, Analytical calculation of minimum miscibility pressure.. *Fluid Phase Equilibria*, **139** (1997), 101–124.

[40] H. Yuan, R.T. Johns, Simplified method for calculation of minimum miscibility pressure or enrichment. *SPE J.,* **10** (2005), 416–425.